3424–3432 *Nucleic Acids Research, 1998, Vol. 26, No. 14*

Topological complexity of different populations of pBR322 as visualized by two-dimensional agarose gel electrophoresis

L. Martín-Parras[+], I. Lucas[1], M. L. Martínez-Robles, P. Hernández, D. B. Krimer, O. Hyrien[1] and J. B. Schvartzman*

Departamento de Biología Celular y del Desarrollo, CIB (CSIC), Velázquez 144, 28006 Madrid, Spain and [1]Génétique Moléculaire, Departement de Biologie, Ecole Normale Supérieure, 46 rue d'Ulm, 75230 Paris Cedex 05, France

Received February 18, 1998; Revised and Accepted March 10, 1998

ABSTRACT

Neutral/neutral two-dimensional (2D) agarose gel electrophoresis was used to investigate populations of the different topological conformations that pBR322 can adopt *in vivo* in bacterial cells as well as in *Xenopus* egg extracts. To help in interpretation and identification of all the different signals, undigested as well as DNA samples pretreated with DNase I, topoisomerase I and topoisomerase II were analyzed. The second dimension of the 2D gel system was run with or without ethidium bromide to account for any possible changes in the migration behavior of DNA molecules caused by intercalation of this planar agent. Finally, DNA samples were isolated from a recA$^-$ strain of *Escherichia coli*, as well as after direct labeling of the replication intermediates in extracts of *Xenopus laevis* eggs. Altogether, the results obtained demonstrated that 2D gels can be readily used to identify most of the complex topological populations that circular molecules can adopt *in vivo* in both bacteria and eukaryotic cells.

INTRODUCTION

Two-dimensional (2D) agarose gel electrophoresis has been successfully used to analyze DNA replication intermediates (RIs) in both prokaryotes and eukaryotes (1–5). One advantage of this method is that it allows identification of the complete population of RIs for any given DNA fragment. In short, during the first dimension of a 2D gel system, restriction fragments are separated mainly according to their mass. To accomplish this task, the first dimension is run in a relatively low percentage agarose gel at low voltage. The conditions for the second dimension, however, are designed to force the geometry and complexity of DNA molecules to play an important role in their migration behavior. For this reason, the second dimension, which is run perpendicular to the direction of the first dimension, takes place in a relatively high percentage agarose gel at high voltage and in the presence of a DNA intercalating agent, namely ethidium bromide. The final result is that RIs are separated mainly according to their mass (or replication extent) during the first dimension and according to their mass and shape during the second dimension (1,2).

For circular DNA molecules, it is well known that they can adopt many different conformations and RIs are not the only population that exist in a cell *in vivo*. Monomers, multimers and different kinds of catenanes and knotted forms have been identified and characterized by different methods (6–17). The conditions used for conventional agarose gel electrophoresis are sufficient to analyze linear DNA fragments as well as to separate supercoiled circular DNA molecules from their nicked counterparts. However, they do not allow a detailed analysis of chromosome-sized DNA molecules or complex forms, such as RIs, knotted molecules or catenanes (18–23).

A different 2D gel method (chloroquine 2D gels) has proven very powerful in resolving topoisomers of covalently closed circular (CCC) plasmid populations (24). In this method, the second dimension electrophoresis is also run perpendicular to the direction of the first dimension. The conditions used for the first and the second dimensions are identical except for the concentration of a DNA intercalating agent, chloroquine, which alters the topology of CCC forms. Chloroquine 2D gels, however, do not allow identification of all the different topological forms that plasmids can adopt *in vivo*, since open circular (OC), linear and branched forms all tend to migrate along the diagonal of the gel and are not resolved from each other (25).

When neutral/neutral 2D gels (1) were used to analyze undigested circular molecules, it was found that complex topological forms migrate with different mobility in both the first and second dimensions. It was also found that besides Cairns (θ-like) RIs, supercoiled (CCC) and OC forms of unreplicated monomers and multimers as well as catenanes could be readily identified (1,26,27). However, no systematic analysis of the

*To whom correspondence should be addressed. Tel: +34 91 564 4562; Fax: +34 91 564 8749; Email: cibjb21@fresno.csic.es

[+]Present address: Institut de Génétique et de Biologie Moléculaire et Cellulaire (IGBMC), Strasbourg, France

migration behavior in 2D gels of these complex topological populations has been carried out so far.

The principal aim of the present work was to investigate the migration behavior in 2D gels of all the different topological populations that exist *in vivo* and could be identified for a bacterial plasmid, pBR322, both in *Escherichia coli* as well as in a eukaryotic system, namely *Xenopus* egg extracts.

MATERIALS AND METHODS

Bacterial strains and culture medium

The *E.coli* strains used in this study were RYC1000 (kindly provided by F.Moreno) and CSH50, transfected with pBR322 DNA. Cells were grown at 37°C in LB medium containing 50 μg/ml ampicillin and 12.5 μg/ml tetracycline.

Isolation of plasmid DNA from bacterial cells

Plasmid DNA isolation from bacterial cells was adapted from the neutral method developed by Clewell and Helinski (28). Cells from overnight 1 l cultures were diluted 40-fold into fresh LB medium, grown at 37°C to exponential phase (A_{600} = 0.4–0.6), quickly chilled and centrifuged. Cells were washed with 20 ml 0.9% (w/v) NaCl, harvested by centrifugation and resuspended in 5 ml 25% (w/v) sucrose, 0.25 M Tris–HCl (pH 8.0). Lysozyme (10 mg/ml) and RNase A (100 mg/ml) were added and the suspension was kept on ice for 5 min. Cell lysis was achieved by adding 8 ml lysis buffer (1% v/v Brij-58, 0.4% w/v sodium deoxycholate, 63 mM EDTA, pH 8.0, 50 mM Tris–HCl, pH 8.0). The lysate was centrifuged at 20 000 *g* for 60 min in order to pellet the cell DNA and other bacterial debris. Plasmid DNA was recovered from the supernatant and precipitated by adding 2–3 vol 25% (w/v) polyethylenglycol 6000 and 1.5 M NaCl. After centrifugation, the DNA in the pellet was dissolved in 5 ml TE buffer (10 mM Tris–HCl, pH 8.0, and 1 mM EDTA, pH 8.0) and digested with proteinase K (100 mg/ml) in 1 M NaCl, 10 mM Tris–HCl (pH 9.0), 1 mM EDTA (pH 9.0) and 0.1% (w/v) SDS at 65°C for 20 min. Proteins were extracted with 10 mM Tris–HCl (pH 8.0)-equilibrated phenol, phenol/chloroform/isoamyl alcohol (25:24:1) and chloroform/isoamyl alcohol (24:1). The DNA was precipitated with ethanol and resuspended in distilled water.

Digestion of plasmid DNA with DNase I

pBR322 DNA was digested with DNase I (Boehringer-Mannheim) in the presence of ethidium bromide (27), to convert all the supercoiled circular DNA (CCC forms) into nicked circular (OC forms) DNA, as determined by standard gel electrophoresis. An aliquot of 0.5 μg CCC DNA was treated with 8 U/ml DNase I in 100 mM sodium acetate (pH 5.0), 5 mM $MgCl_2$, 100 μg/ml ethidium bromide at 14°C for 30 min. Digestion was stopped by addition of 30 mM EDTA (pH 8.0) followed by phenol/chloroform/isoamyl alcohol (25:24:1 v/v) extraction.

Replication of plasmid DNA in *Xenopus* egg extracts

pBR322 DNA was prepared from the $recA^+$ BL21 strain by standard alkaline lysis and cesium chloride gradient centrifugation (29). Replication-competent extracts from unfertilized *Xenopus* eggs (30) were prepared and used as described elsewhere (3), with minor modifications. The electric shock activation step, which we found unnecessary, was omitted and an ATP regeneration system was added (31). Addition of [α-^{32}P]dATP to the extract allowed direct labeling of all the replication products. After incubation in this extract, plasmid DNA was isolated by digestion with RNase A and proteinase K, phenol/chloroform extraction and ethanol precipitation as described elsewhere (3).

Treatments of *E.coli* plasmids with topoisomerase I and II

An aliquot of 1 μg plasmid DNA isolated from *E.coli* was resuspended in 120 μl topoisomerase (topo) I or topo II buffer (Amersham) and incubated at 37°C with 13–15 U/μg calf thymus topo I or at 30°C with 100 U/μg *Drosophila melanogaster* topo II respectively. Aliquots were removed after 30 s or 30 min for topo I and 30 s or 15 min for topo II. After removal, the topo I reaction was stopped by pipetting into a tube containing 1.25% SDS. The topo II reaction was stopped by adding 1 mM EDTA and 0.11% SDS.

Treatment with topo I of plasmids incubated in *Xenopus* extracts

Aliquots of 100 ng plasmid DNA isolated from egg extracts were resuspended in 80 μl topo I buffer (Amersham) and incubated at 37°C with 50 U calf thymus topo I for 3 h. The mixture was precipitated with ethanol, resuspended in TE and loaded into the first electrophoresis gel.

Two-dimensional agarose gel electrophoresis

The first dimension electrophoresis was in a 0.4% (w/v) agarose gel in TBE buffer (89 mM Tris–borate, 2 mM EDTA) at 0.6 V/cm at room temperature for 34 h for the autoradiograms shown in Figures 1, 3 and 4 or at 1 V/cm at room temperature for 18 h for the autoradiograms shown in Figures 2 and 5. The lane containing the λ DNA/*Hin*dIII marker sizes was excised, stained with 0.5 μg/ml ethidium bromide and photographed. The second dimension was in a 1 (for Figs 1, 3 and 4) or 1.1% (for Figs 2 and 5) agarose gel. The dissolved agarose was poured around the excised lane from the first dimension and electrophoresis was carried out at a 90° angle with respect to the first dimension. Second dimension electrophoresis was performed in TBE buffer with or without 0.5 (for Figs 1, 3 and 4) or 0.3 μg/ml (for Figs 2 and 5) ethidium bromide at 5 V/cm for 7 (for Figs 1, 3 and 4) or for 8 h (for Figs 2 and 5) in a 4°C cold room using recirculating buffer.

Southern transfer and hybridization

For the autoradiograms shown in Figures 1, 3 and 4, after electrophoresis the gels were washed twice for 15 min in 50 mM HCl and twice for 15 min in 0.5 M NaOH containing 1 M NaCl, followed by a 60 min wash in 1 M Tris–HCl (pH 8.0), 1.5 M NaCl. The DNA was transferred to Optibind nitrocellulose-supported membranes (Schleicher & Schuell Inc.) in 10× SSC (0.15 M NaCl, 15 mM sodium citrate) for 16–18 h and the membranes were baked at 80°C for 2 h. Prehybridization was carried out in 50% (v/v) formamide, 5× SSC, 5× Denhardt's solution and 250 mg/ml sonicated salmon testes DNA. Hybridization was performed at 42°C for 24–48 h in the same mixture plus 10% (w/v) dextran sulfate with 10^6 c.p.m./ml pBR322 DNA labeled with [α-^{32}P]dCTP by random priming. After hybridization, the membranes were washed twice for 15 min in 2× SSC and 0.1% SDS at room temperature, followed by 2–3 washes in 0.1× SSC and 0.1% SDS at 55°C for 30 min each time. Exposure of XAR-5 films

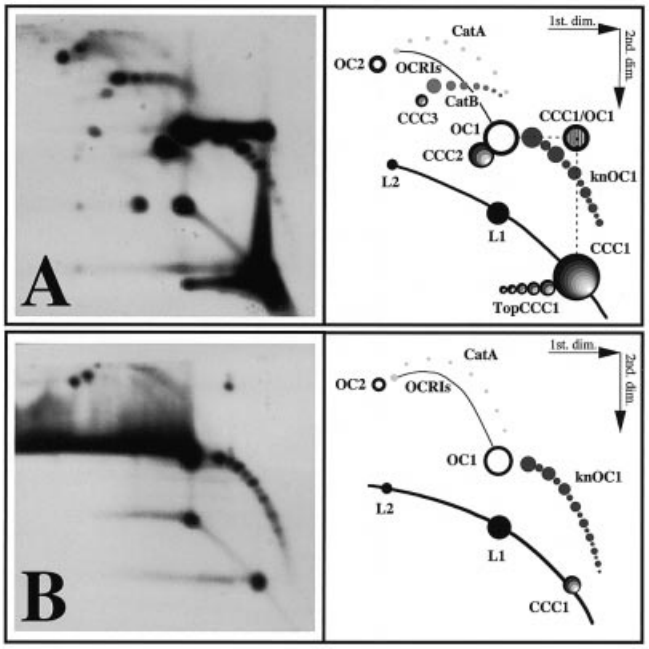

Figure 1. Two-dimensional agarose gel electrophoresis of pBR322 DNA isolated from the recA⁻ strain RYC1000 of *E.coli*. The second dimension occurred in the presence of 0.5 μg/ml ethidium bromide. After Southern blotting, the membrane was hybridized with radioactively labeled pBR322 DNA used as probe. A photograph of the autoradiogram is shown to the left and a diagrammatic interpretation is shown to the right. (**A**) Undigested DNA. (**B**) DNA briefly treated with DNase I in the presence of ethidium bromide just before electrophoresis. L, linear molecules; CCC, covalently closed circles; OC, open circles; the numbers refer to the multimeric state (1, monomers, 2, dimers, 3, trimers, etc.); CCC/OC, DNA molecules that migrated as covalently closed circles during the first dimension, were subsequently nicked and migrated as relaxed circles during the second dimension; RIs, replication intermediates; CatA, catenanes formed by two relaxed circles; CatB, catenanes formed by one relaxed and another covalently closed circle; knOC, relaxed circles with at least one knot and a variable number of nodes; TopCCC, covalently closed circles with different levels of supercoiling.

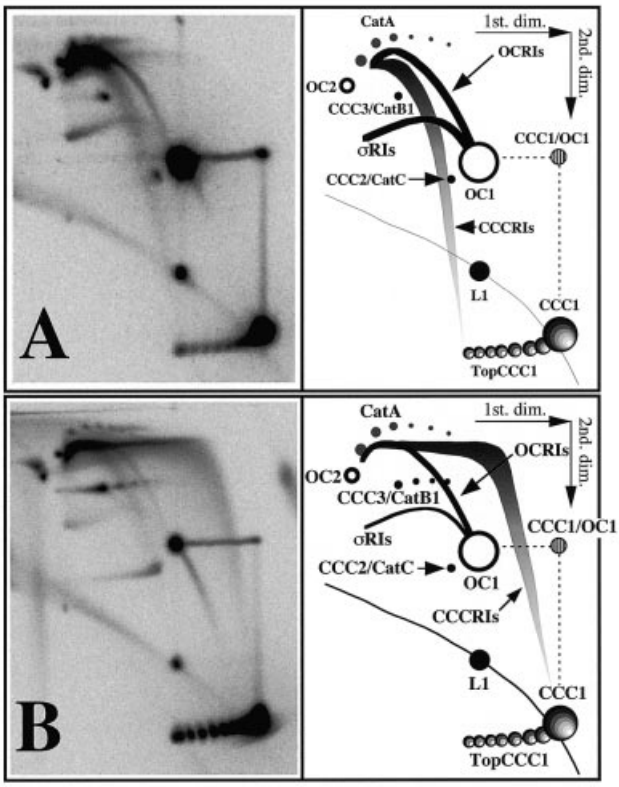

Figure 2. Two-dimensional agarose gel electrophoresis of pBR322 DNA incubated in *X.laevis* egg extracts. The second dimension occurred in the presence of 0.3 μg/ml ethidium bromide. The result of two independent experiments are shown in (**A**) and (**B**). Replicating pBR322 molecules were directly labeled during replication due to the presence of [α-^{32}P]dATP in the extract. L, linear molecules; CCC, covalently closed circles; OC, open circles; the numbers refer to the multimeric state (1, monomers, 2, dimers); CCC/OC, DNA molecules that migrated as covalently closed circles during the first dimension, were subsequently nicked and migrated as relaxed circles during the second dimension; CCCRIs, covalently closed replication intermediates with different levels of supercoiling; OCRIs, relaxed replication intermediates; σRIs, replication intermediates with one broken fork; CatA, catenanes formed by two relaxed circles; CatB, catenanes formed by one relaxed and another covalently closed circle; CatC, catenanes formed by two covalently closed circles; TopCCC, covalently closed circles with different levels of supercoiling.

(Kodak) was carried out at –80°C with intensifying screens for 1–3 days. For the autoradiograms shown in Figures 2 and 5, after electrophoresis the gel was blotted in 0.4 N NaOH onto Hybond-N$^+$ (Amersham). The membranes were directly exposed to a Fuji BAS MP 2040S imaging plate for 3 days and the images were read on a Fuji BAS 1000 phosphorimager using the TINA software.

RESULTS AND DISCUSSION

Plasmid DNA was isolated from exponentially growing RYC1000 bacteria, a recA⁻ strain, and analyzed by neutral/neutral (N/N) 2D agarose gel electrophoresis (Fig. 1A). The first dimension was performed without ethidium bromide but the second dimension occurred in the presence of 0.5 μg/ml ethidium bromide in order to magnify the role of both geometry and complexity of DNA molecules in their mobility through the gel. Because the neutral DNA extraction method was specific for plasmid DNA and the signals detected corresponded to molecules that specifically hybridized to a pBR322 DNA probe, we concluded that the complex patterns detected in the autoradiogram shown in Figure 1A corresponded to different populations of pBR322 that existed *in vivo* in the bacterial cells.

Identification of supercoiled and open circular forms

To help us in the interpretation and identification of all the different signals, an aliquot of the same DNA was digested with DNase I before being analyzed (Fig. 1B). The extent of DNase I treatment was the minimum required to transform most of the supercoiled molecules (CCC forms) into relaxed molecules (OC forms), as determined for a DNA sample analyzed by conventional electrophoresis in ethidium bromide stained gels. It was assumed that those signals that disappeared or became fainter after the nuclease treatment corresponded to supercoiled (CCC) forms. Also, new signals and others that increased in intensity after the DNase I treatment corresponded to relaxed (OC) forms. As shown in Figure 1A, the signals detected by the pBR322 DNA

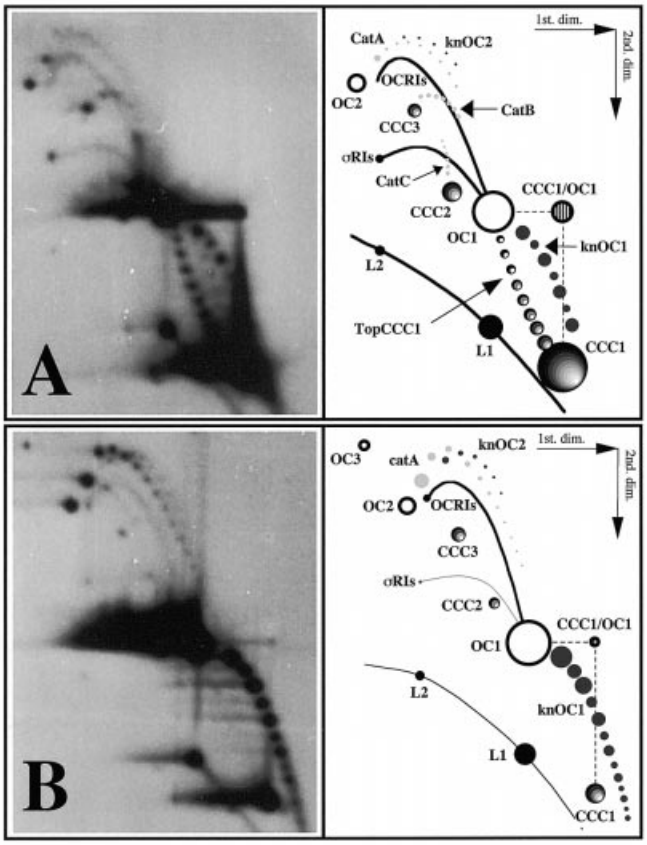

Figure 3. Two-dimensional agarose gel electrophoresis of pBR322 DNA isolated from the recA⁻ strain RYC1000 of *E.coli*. The first as well as the second dimensions were run without ethidium bromide. After Southern blotting, the membrane was hybridized with radioactively labeled pBR322 DNA used as probe. (**A**) Undigested DNA. (**B**) DNA briefly treated with DNase I just before electrophoresis. L, linear molecules; CCC, covalently closed circles; OC, open circles; the numbers refer to the multimeric state (1, monomers; 2, dimers; 3, trimers, etc.); CCC/OC, DNA molecules that migrated as covalently closed circles during the first dimension, were subsequently nicked and migrated as relaxed circles during the second dimension; OCRIs, replication intermediates with at least one nick in the unreplicated portion; σRIs, replication intermediates with one broken fork; CatA, catenanes formed by two relaxed circles; CatB, catenanes formed by one relaxed and another covalently closed circle; CatC, catenanes formed by two covalently closed circles; knOC, relaxed circles with at least one knot and a variable number of nodes; knCCC, covalently closed circles with at least one knot and a variable number of nodes; TopCCC, covalently closed circles with different levels of supercoiling.

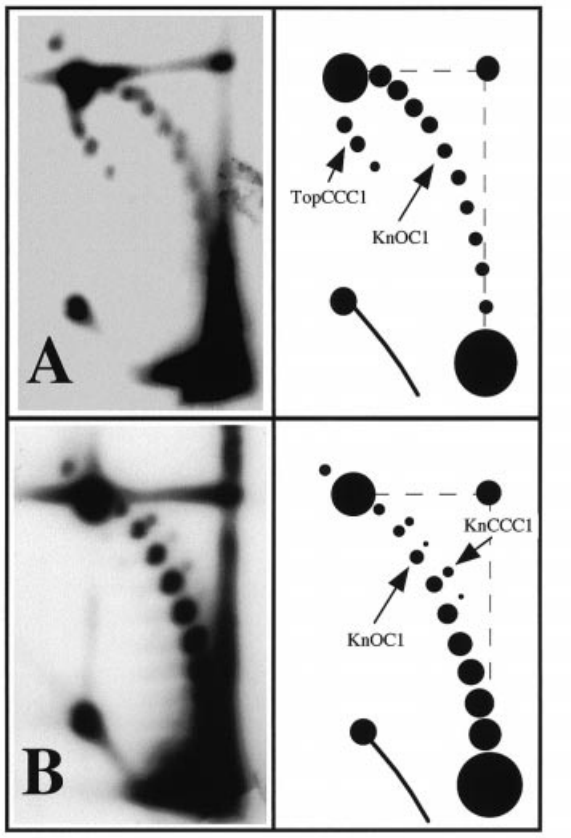

Figure 4. Two-dimensional agarose gel electrophoresis of pBR322 DNA isolated from the recA⁻ strain RYC1000 of *E.coli* after treatments with eukaryotic topos I and II. In both cases, the first as well as the second dimensions were run without ethidium bromide. After Southern blotting, the membrane was hybridized with radioactively labeled pBR322 DNA used as probe. (**A**) DNA treated with topo I. (**B**) The same DNA treated with topo II. knOC, relaxed circles with at least one knot and a variable number of nodes; knCCC, covalently closed circles with at least one knot and a variable number of nodes; TopCCC, covalently closed circles with different levels of supercoiling.

probe were very heterogeneous, suggesting the existence of several populations. Comparison of the results obtained from untreated (Fig. 1A) and DNase I-treated (Fig. 1B) samples allowed us to determine which signals corresponded to supercoiled and relaxed forms. These molecules are referred to as CCC (for covalently closed circles) and OC (for open circles). The number that follows (1, 2, 3, etc.) refers to monomers, dimers, trimers and higher oligomers respectively.

The replication products generated by incubation of pBR322 in a *Xenopus* egg extract in the presence of [α-^{32}P]dATP and analyzed using 2D agarose gel electrophoresis conditions similar to those used in Figure 1 are shown in Figure 2. Purified DNA of any source replicates in these extracts in a semi-conservative, cell cycle-regulated fashion, regardless of the origin of the input DNA (3,30). By comparison with Figure 1A, we concluded that the two major spots of replication products corresponded to OC1 and CCC1 monomer plasmids. In addition, OC2 dimer and CCC2 dimer and CCC3 trimer spots were also identified.

Besides the supercoiled and open circular monomers and oligomers of pBR322, the autoradiograms depicted in Figures 1 and 2 show other continuous and discontinuous signals. In some cases the resolution obtained was not sufficient to identify the topology of these molecules. Ethidium bromide is a planar molecule that intercalates between the stacked bases of DNA (32). In negatively supercoiled forms this intercalation causes unwinding of superhelical turns (33). Indeed, a sufficiently high concentration of ethidium bromide may absorb all negative DNA supercoiling and even add some positive supercoiling to DNA circles. Our principal goal, however, was to identify all the naturally occurring pBR322 DNA molecules and the use of an intercalating agent could be masking some of the existing plasmid populations. On the other hand, this peculiar property of ethidium bromide could be used to facilitate identification of some

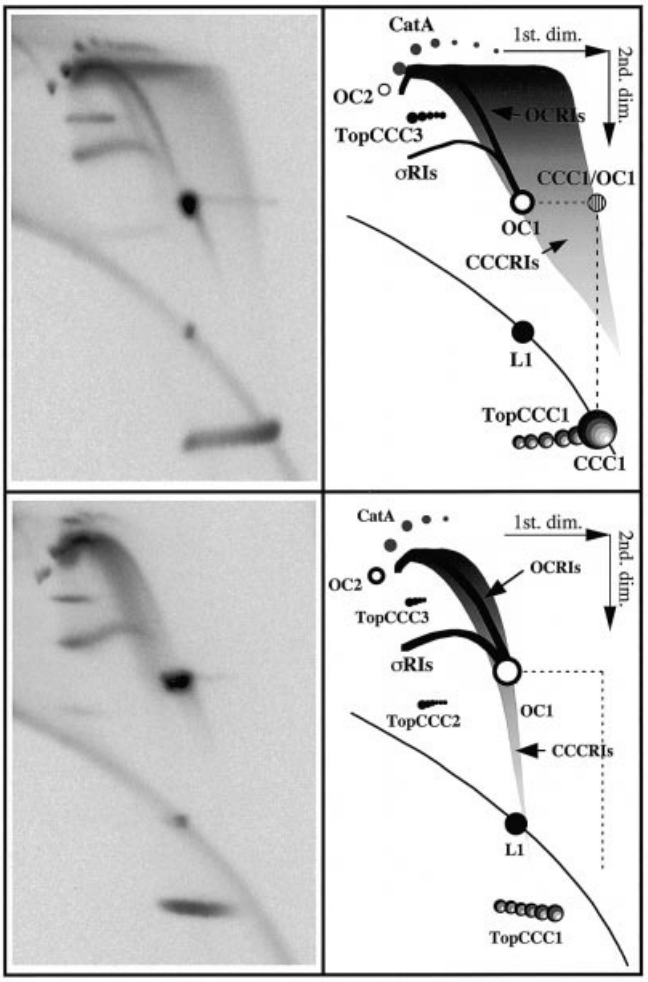

Figure 5. Two-dimensional agarose gel electrophoresis of pBR322 DNA isolated from *Xenopus* egg extracts, followed by complete relaxation by calf thymus topo I. The second dimension occurred in the presence of 0.3 μg/ml ethidium bromide. Replicating pBR322 molecules were directly labeled during replication due to the presence of [α-^{32}P]dATP in the extract. L, linear molecules; CCC, covalently closed circles; OC, open circles; the numbers refer to the multimeric state (1, monomers; 2, dimers); CCC/OC, DNA molecules that migrated as covalently closed circles during the first dimension, were subsequently nicked and migrated as relaxed circles during the second dimension; CCCRIs, covalently closed replication intermediates with different levels of supercoiling; OCRIs, relaxed replication intermediates; σRIs, replication intermediates with one broken fork; CatA, catenanes formed by two relaxed circles; CatB, catenanes formed by one relaxed and another covalently closed circle; CatC, catenanes formed by two covalently closed circles; TopCCC, covalently closed circles with different levels of supercoiling.

stereoisomers. For this reason, we decided to repeat one of the experiments, but this time using a 2D agarose gel system in which both dimensions were run in the absence of ethidium bromide. Figure 3 shows the results obtained when an untreated DNA sample (Fig. 3A) and a DNase I-treated sample (Fig. 3B) were analyzed as previously described. A complex hybridization pattern was obtained corresponding to unique signals as well as continuous and discontinuous arcs.

Identification of knotted forms

The series of signals observed in Figures 1A and B and 3A and B that form a discontinuous arc extending downward and to the right from the OC1 spot, labeled knOC1, was interpreted as a population of pBR322 stereoisomers corresponding to monomers which differ in their number of intramolecular links. This interpretation is based on several observations. First, the signals did not form a continuous but a discontinuous arc. Therefore, they were not intermediates of a continuous process such as, for example, DNA replication. During the first dimension these molecules migrated to positions extending between OC1 and CCC1, indicating that they were monomers that differed in their topology. When the DNA was digested with DNase I (Figs 1B and 3B) these signals did not disappear, but rather increased in intensity. This means that the molecules responsible were not supercoiled. There is only one population that fulfills the restrictions of not being supercoiled monomers and still existing as a series of stereoisomers. It corresponds to monomeric knotted and relaxed circles with different numbers of nodes (9).

There are several lines of evidence that further support this assignment. First, in one-dimensional gel systems not very different from our first dimension gels, relaxed and knotted plasmid molecules migrated diversely according to their number of nodes (34 and references therein). Second, it has been shown that in *E.coli* topo I deletion mutants, the presence of the region that encodes resistance to tetracycline (*tet*) is responsible for high levels of plasmid DNA knotting (15). As these knotted forms have the same primary structure as unknotted DNA molecules, it was concluded that they were not the product of intramolecular recombination (15), as occurs in other systems where knotted molecules were found to be the result of site-specific recombination mediated by the Tn*3* resolvase (35). Inactivation of the *tet* promoter or inversion of the *tet* gene was found to reduce the population of knotted molecules, but did not abolish it (15). It was proposed that in *E.coli* cells, these knotted forms are generated by a DNA gyrase reaction (14,36). However, low concentrations of coumermycin, a DNA gyrase inhibitor, not only do not abolish plasmid knotting but rather increase it. In contrast, rifampicin, an inhibitor of RNA synthesis initiation, does inhibit knotting (15). Although the mechanism for this unusual knotting of pBR322 DNA in *E.coli* cells is not yet fully understood, the primary structure of the DNA in the region and transcription of the *tet* gene certainly play an important role (15). Third, another remarkable observation was that the knOC1 arc observed in Figures 1 and 3 displayed a peculiar alternation of signals with different hybridization intensities. This observation is in agreement with the results previously reported by others (14,15), suggesting that in *E.coli* cells pBR322 molecules with an odd number of nodes seem to be generated in a predominant fashion. An alternative hypothesis is that the difference in intensity observed for knOC1 in Figures 1 and 4 might reflect the relative abundance of the torus and twist families of knotted molecules in *E.coli* cells. Indeed, high resolution gels have been successfully used to separate torus- and twist-type knots having the same minimal numbers of crossings (34,37,38). A more detailed investigation is needed to fully understand this observation. A presumptive arc of knotted plasmid dimers, labeled knOC2, was also detected in Figure 3. This arc migrated close to the arc of nicked catenated dimers (CatA; see below).

Identification of relaxed knotted forms and the increase in signal intensity observed for these molecules in the DNase

I-treated samples (Figs 1B and 3B) suggested the existence of supercoiled knotted forms. These forms should migrate from positions close to the OC1 spot to positions close to the CCC1 spot and even further down, due to the high compaction expected for these molecules produced by both the superhelical turns and the intramolecular links. In fact, there might be more than one family of knCCC1 and the faint arc of spots migrating between TopCCC1 and knOC1 in Figure 3A could correspond to one of these families. Treatment of the DNA sample with DNase I led to disappearance of this signal (Fig. 3B), which may have contributed to the gain in signal intensity observed for the knOC1 arc. Migration of knCCC1 molecules is discussed below in a more extensive manner.

In contrast to the abundance of knotted forms in the samples isolated from *E.coli* cells (Figs 1 and 3), neither open circular nor supercoiled knotted forms were detected in the DNA replicated in interphase *Xenopus* egg extracts (Fig. 2). In this particular experiment, unreplicated plasmid molecules remained unnoticed, since only the replication products were labeled in the extract and thus detected in the autoradiogram. Nevertheless, knotted forms were not detected even when the blot was hybridized with a pBR322-labeled probe, which allows identification of all plasmid molecules from the extract (data not shown). In contrast to these findings, knotting of plasmid DNA was observed in extracts prepared from metaphase-arrested *Xenopus* eggs by one- and two-dimensional chloroquine gel electrophoresis (39). The absence of knotted forms in the interphase egg extracts was not attributable to a deficiency in topo II, since this enzyme is abundant in *Xenopus* eggs and interphase egg extracts (40–42). Further work is required to determine whether the difference between our results and those of Sanchez *et al*. (39) is due to differences in extract preparation or reaction conditions or to an actual cell cycle regulation of DNA knotting.

Nevertheless, it is worth noting that topo II activity is 4- to 5-fold higher in mitotic extracts compared with interphase extracts (40). A higher ratio of active topo II to plasmid molecules favors knotting *in vitro* (7). The difference in topo II activity, or a different conformation of the chromatin template, may thus account for the different behavior of mitotic and interphase extracts. Furthermore, the lack of plasmid knotting in interphase extracts is consistent with the absence of self-knots in interphase chromosome fibers (43–46) and the presence of knots in mitotic extracts supports a model that implies self-knotting of chromosomal fibers as a mechanism for topo II-driven mitotic chromosome condensation (45).

Identification of molecules with different levels of supercoiling

The discontinuous arc of signals designated TopCCC1 in Figure 3A was interpreted as topoisomers of the monomeric form. This signal corresponded to a population of monomers, since the arc spanned between the positions where OC1 and CCC1 migrated during the first dimension. The signal disappeared after treatment with DNase I (Fig. 3B), indicative of its covalently closed nature. The discontinuous nature of the arc indicated that the individual molecular species differed in their linking number. The spots increased in intensity as they approached CCC1. Finally, intercalation of ethidium bromide significantly affected the migration behavior of these molecules (compare Figs 1A and 3A). When the second dimension occurred in the presence of ethidium bromide, TopCCC1 produced a rather horizontal signal extending leftward and slightly downward from the spot generated by CCC1 (Figs 1A and 2). This signal was also formed by several discrete spots (Fig. 2 and lower exposures of Fig. 1A; not shown) and it disappeared after DNase I treatment (Fig. 1B). All these observations led us to conclude that this TopCCC1 arc indeed corresponded to a population of monomeric supercoiled molecules that differed in their linking number.

Why does a family of topoisomers migrate differently depending on whether or not ethidium bromide was present during the second dimension electrophoresis? In the absence of ethidium bromide, the fully relaxed topoisomer ($Lk = Lk_0$) is the least compact and migrates the slowest, close to the OC species. Topoisomers with increasing linking number differences ($\Delta Lk = Lk - Lk_0$), either positive or negative, have an increasingly compact configuration and migrate faster. For this reason, when the two consecutive electrophoreses were run in the absence of ethidium bromide, topoisomers displayed the curved diagonal arc observed in Figure 3A. As discussed above, ethidium bromide is a planar molecule that intercalates between the stacked bases of DNA (32). In negatively supercoiled molecules this intercalation causes unwinding of the superhelical turns (33). Due to covalent closure, all topoisomers, including that with the highest linking number, would absorb much less ethidium bromide than the relaxed circle and would migrate faster. At high ethidium bromide concentrations, all topoisomers will be positively supercoiled. The more negatively supercoiled a topoisomer was before addition of ethidium bromide, the less positively supercoiled it will become upon interaction with ethidium bromide. In consequence, the topoisomer with the lowest *Lk* will be the fastest migrating species in the second dimension. This explains why when ethidium bromide was present, the TopCCC1 signal was not horizontal but extended leftward and slightly downward from the spot generated by CCC1 (Figs 1A and 2). However, when the second dimension occurred in the absence of ethidium bromide, TopCCC1 migrated forming an arc extending between OC1 and CCC1 (Fig. 3A).

In order to confirm the assignments made for knotted and supercoiled forms, we decided to treat the samples with topos I and II before analyzing them in 2D gels. Calf thymus topo I can relax both positively and negatively supercoiled DNAs, but does not affect catenanes and knotted forms unless one strand of the duplex contains a nick or a gap (25). Eukaryotic topo II also can relax positively as well as negatively supercoiled DNAs. Besides this, duplex molecules without nicks, gaps or supercoils can be catenated, decatenated, knotted and unknotted by topo II (25). Figure 4 shows the results obtained after treating pBR322 DNA isolated from *E.coli* with calf thymus topo I (Fig. 4A) or II (Fig. 4B) for 30 s. In both cases, the second dimension electrophoresis was run without ethidium bromide. Only the regions of the gel where knotted and supercoiled monomers migrated are depicted in the autoradiograms. As expected, both enzymes eliminated almost all the signals that were identified as TopCCC1 in the untreated samples (see Figs 1 and 3), although topo II was more effective than topo I in this respect. The appearance of the knOC1 arc also changed. In particular, the intensity and sharpness of each individual spot increased notably after treatment with topo II (Fig. 4B). Moreover, the alternation of signals with different hybridization intensities that was observed for the untreated sample (Fig. 3A) as well as for the sample digested with DNase I (Fig. 3B) was not detected after treatment with topo II (Fig. 4B). Finally, the intensity of the spots forming this arc increased downward after topo II treatment, whereas it was exactly the reverse in the

untreated sample, as well as in the sample digested with DNase I (see Fig. 3A and B). These differences are likely due to the capacity of topo II to unknot as well as to knot relaxed unnicked DNA circles.

As previously mentioned, identification of relaxed knotted forms and the increase in signal intensity observed for these molecules in the DNase I-treated samples (Figs 1B and 3B) suggested the existence of supercoiled knotted forms. Two minor signals that meet these predictions were detected: (i) a faint arc of spots migrating between TopCCC1 and knOC1 in Figure 3A which disappeared upon treatment of the DNA sample with DNase I (Fig. 3B) and which was not detected when ethidium bromide was present in the second dimension (Fig. 1A), perhaps due to co-migration with TopCCC1 species; (ii) a faint arc of spots migrating slightly above knOC1 in Figure 4B which appeared upon treatment of the DNA sample with topo II (see below). Both signals could correspond to minor knCCC species.

A prominent spot that migrated at about the same position as the CCC1 spot was still detected after the samples were treated with topo I or II (Fig. 4). Although both enzymes eliminated almost all the signals identified as TopCCC1 in the untreated samples, a strong signal persisted at about the same position as the CCC1 spot. This should correspond to molecules that have approximately the same compactness as CCC1 even after relaxation of supercoils by topos I and II. The simplest interpretation is that they correspond to knotted molecules with such a high degree of knotting that they are sufficiently compact to migrate at maximum speed in both gel dimensions.

For plasmids incubated in *Xenopus* extracts, several changes were also observed after complete relaxation by topo I and 2D gel analysis where the second dimension occurred in the presence of ethidium bromide (see Fig. 5). The negatively supercoiled monomer plasmids (TopCCC1), which in the untreated sample migrated to the left of the CCC1 spot and tilted downward to the left, after topo I treatment were converted into a different range of spots which now migrated tilted to the right. This is shown by the inclination of the topoisomer ladder before and after topo I treatment. Note also that CCC1 was no longer detected after topo I treatment. Other changes in the 2D gel patterns observed after treatment with topo I are discussed in the next section.

Identification of DNA RIs

As shown in Figures 1–3, several continuous hybridization signals were detected migrating between the OC1 and OC2 positions in the first dimension. The only process that can give rise to a continuous arc is DNA replication. Consistently, these continuous arcs were prominent in the *Xenopus* experiment (Fig. 2), where RIs were selectively labeled, whereas they were fainter in the *E.coli* experiments (Figs 1 and 3), where pBR322 DNA was detected by hybridization and RIs were only a minor fraction of all plasmid molecules in the sample.

One of these arcs, labeled OCRIs, was consistently detected in all the autoradiograms. It started at the OC1 spot and terminated close to the CatA1 spot (see below). Neither DNase I (Figs 1B and 3B) nor topo I (Fig. 5) were able to eliminate this arc, suggesting that the molecular species responsible contained no supercoils. Therefore, we postulate that this arc was generated by open circular Cairns intermediates (47). This interpretation is consistent with the observations made for SV40 (8,9) and for the 2 μm plasmid of *Saccharomyces cerevisiae* (1,26) by one- and two-dimensional agarose gel electrophoresis respectively.

Another continuous signal was clearly detected in *Xenopus* (Fig. 2) that was almost negligible in *E.coli* (Figs 1 and 3). This arc was not well defined, but described a rather broad smear starting above TopCCC1 and extended upward to variable sites to the right of the OC2 spot. This smeared signal was interpreted as generated by supercoiled RIs and was labeled CCCRIs. In the particular experiment shown in Figure 2A, the left-most part of the smear was the most prominent, but in other experiments (see Fig. 2B) the right-most part was predominant, generating a pattern that resembled that found by Brewer and co-workers (26) for the supercoiled Cairns RIs of the 2 μm plasmid of *S.cerevisiae*. Although a close inspection shows a continuum of RIs between the left-most and righ-most positions (Fig. 2B), only the lateral, more intense parts of the broad smears of CCCRIs have been pictured in the diagramatic interpretations (Fig. 2, right). In Figure 5, the broad continuum of RIs, which we call the 'Niagara falls' pattern, was particularly obvious in the untreated DNA sample. Upon relaxation with topo I, all these CCCRIs migrated to the most leftward position. The signal was also more intense, indicating that the RIs that were initially spread throughout the width of the gel, upon relaxation of supercoils now concentrated into a more restricted area of the gel.

Therefore, we interpret the variations in migration behavior of CCCRIs in untreated DNA samples as due to different rates of DNA unlinking during replication. Migration of a supercoiled Cairns intermediate should depend on both mass (i.e. replication extent) and topology (i.e. residual *Lk* of the two parental strands). The residual *Lk* should diminish during replication and come close to 0 at termination. However, the exact relationship between mass and topology will depend on the lag between fork progression and the action of topoisomerases to release the positive supercoiling generated by fork progression (48). In addition, variations in replication-coupled chromatin assembly might also have a minor effect on the final topology of RIs.

It is still unknown whether completion of replication can occur without unwinding, giving rise to two fully mature but catenated circles, or only after the last helical turns are completely unwound, generating two non-catenated circles (49). Different modes for completion of replication may predominate in different organisms. A fine analysis of the migration behavior of the latest CCCRIs could shed new light on this particular problem, but falls outside the scope of the present paper.

CCCRIs were almost negligible in the autoradiograms corresponding to samples isolated from *E.coli* cells. Only the top of the left-most curve of CCCRIs was detected, barely (Fig. 1A). The DNA purified from *Xenopus* egg extracts, on the other hand, was selectively labeled during replication in the extract and the DNA sample analyzed by Brewer and co-workers (26) was extracted from yeast cells that had been synchronized in S phase of the cell cycle. In our *E.coli* samples, pBR322 DNA was isolated from unsynchronized cells. This may explain the difference in the relative abundance of RIs observed among the three experiments. Furthermore, it is well known that nicks can be easily produced while manipulating DNA during the isolation procedure (50). Therefore, it could be that we observed very few covalently closed RIs in *E.coli* cells simply because the sample was not enriched for RIs and a significant fraction of the CCCRIs that were present could have been nicked during DNA isolation. Persistence of only the latest supercoiled RIs could be due to a

decrease in the target for conversion of CCCRIs into OCRIs by nicking in these late intermediates. Note that nicking of the parental strands in the replicated portion has no effect on plasmid supercoiling, as it does not lead to a change in *Lk* (48).

There was a third continuous 'eyebrow'-shaped signal in Figures 2 and 3 that also migrated between the OC1 and OC2 positions in the first dimension. This arc ended at a conspicuous spot in the case of *E.coli* (Fig. 3) but not in the case of *Xenopus* (Fig. 2). This arc was labeled σRIs. It was unaffected by topo I treatment (Fig. 5). Martín-Parras and co-workers (50) demonstrated that during DNA isolation single-stranded breaks at one fork convert bubbles into branched structures. For a circular molecule this event would lead to a sigma-shaped intermediate. If one considers that the whole population of RIs may suffer this kind of breakage during DNA isolation, a secondary (or artifactual) population of RIs would be expected (50). This population would consist of a DNA circle with a double-stranded tail of increasing length. We postulate that the signal labeled σRIs corresponds to these derivatives of the genuine population of RIs. This observation is in agreement with those made in the case of rolling circle replication analyzed on 2D agarose gels (51,52). Rolling circle intermediates follow the 'eyebrow' path between the 1*n* and 2*n* positions and migrate further upwards and leftwards at higher masses. Such high molecular weight signals were detected neither in *E.coli* cells nor in *Xenopus* egg extracts, consistent with the lack of significant rolling circle replication of pBR322 in these experimental systems. The conspicuous spot at the end of this arc in the case of RIs isolated from *E.coli* (Fig. 4) may result from breakage at one of the forks of late intermediates, which are known to accumulate in *E.coli* (4,5,50).

Identification of catenanes

Some of the most retarded signals in both dimensions that were observed in all the experiments corresponded to various discontinuous arcs that migrated approximately between OC1 and OC2. These arcs were likely to be the catenated products of DNA replication, where the two daughter duplexes were still interlocked by a variable but discrete number of turns (1,8,9,26,49). These signals are labeled CatA, CatB and CatC (Figs 1–3). According to Sundin and Varshavsky (8): CatA corresponds to catenanes in which both circular members are nicked or gapped; CatB is composed of catenanes in which one circular member is nicked or gapped while the other is covalently closed; CatC corresponds to catenanes where both members are covalently closed. Several lines of evidence favor the assignments we made. First, the putative CatA and CatB arcs were made up of discrete spots, defining them as families of stereoisomers (8,9). Second, in the first dimension they migrated approximately between OC1 and OC2. Therefore, they were likely to be double the mass of monomeric forms. Finally, when the second dimension was run in the absence of ethidium bromide, two of the signals disappeared after the DNase I treatment and the intensity of the remaining one significantly increased (Fig. 3A and B). The latter strongly suggests that augmentation of signal strength after DNase I treatment was due to conversion of the CatB and CatC forms into CatA forms, which allowed us to unambiguously identify CatA (Fig. 3A and B). For *Xenopus*, note that the distribution of linkage states of the A and B type catenanes is broader in Figure 2B than in Figure 2A. This, and the different aspect of CCCRIs in the two panels, may be due to a different decatenation activity in the two extracts.

To confirm that the continuous signals described before indeed correspond to RIs while the discontinuous signals corresponded to catenanes, topoisomers and knotted forms, aliquots of the same pBR322 DNA sample analyzed in Figures 1 and 2 were digested with several restriction enzymes that cut only once per molecule and analyzed by 2D agarose gel electrophoresis. The only signals detected in these autoradiograms corresponded to linear forms and the classical bubble, simple and double Y patterns generated by RIs (data not shown). These patterns have already been described by Martín-Parras and co-workers (5). Similar results were obtained for the *Xenopus* samples analyzed in Figures 3 and 5 (3; data not shown). The fact that restriction enzyme digestion converted all catenanes, topoisomers and knotted molecules to linear forms, with the only exception being those corresponding to RIs, further supports our previous interpretations.

In short, we have shown that 2D gels can be readily used to identify most of the complex topological populations that circular molecules can adopt *in vivo* in bacteria as well as in eukaryotic cells. This technique is able to resolve species such as OCRIs, CCCRIs, catenanes and knotted circles, which tend to overlap in standard one-dimensional agarose gel electrophoresis or in chloroquine 2D gels Also, neutral/neutral 2D gels can reveal even subtle changes in the migration behavior of specific molecular species, such as those induced by ethidium bromide. We believe this system will prove useful to investigate the effects of gyrases and topoisomerases and their inhibitors through the use of cell mutants.

ACKNOWLEDGEMENTS

We are grateful to David Santamaría and Enrique Viguera for critical comments and to P.Robles for technical assistance. This work was partially supported by grants 96/0470 and PM95/0016 from the Spanish Fondo de Investigación Sanitaria and Dirección General de Enseñanza Superior respectively and grants from the French CNRS-ATIPE, ARC and LNCC. I.L. was supported by a MENESR fellowship.

REFERENCES

1 Brewer,B.J. and Fangman,W.L. (1987) *Cell*, **51**, 463–471.
2 Friedman,K.L. and Brewer,B.J. (1995) In Campbell,J.L. (ed.), *DNA Replication*. Academic Press, San Diego, CA, Vol. 262, pp. 613–627.
3 Hyrien,O. and Mechali,M. (1992) *Nucleic Acids Res*., **20**, 1463–1469.
4 Kuzminov,A., Schabtach,E. and Stahl,F.W. (1997) *J. Mol. Biol*., **268**, 1–7.
5 Martín-Parras,L., Hernández,P., Martínez-Robles,M.L. and Schvartzman,J.B. (1991) *J. Mol. Biol*., **220**, 843–853.
6 Keller,W. (1975) *Proc. Natl. Acad. Sci. USA*, **72**, 4876–4880.
7 Liu,L.F., Liu,C.C. and Alberts,B.M. (1980) *Cell*, **19**, 697–707.
8 Sundin,O. and Varshavsky,A. (1980) *Cell*, **21**, 103–114.
9 Sundin,O. and Varsharvsky,A. (1981) *Cell*, **25**, 659–669.
10 Dean,F.B., Stasiak,A., Koller,T. and Cozzarelli,N.R. (1985) *J. Biol. Chem*., **260**, 4975–4983.
11 Komiyama,N. and Shishido,K. (1986) *FEBS Lett*., **204**, 269–272.
12 Minden,J.S. and Marians,K.J. (1986) *J. Biol. Chem*., **261**, 11906–11917.
13 Pruss,G.J. and Drlica,K. (1980) *Proc. Natl. Acad. Sci. USA*, **83**, 8952–8956.
14 Shishido,K., Komiyama,M. and Ikawa,S. (1987) *J. Mol. Biol*., **195**, 215–218.
15 Shishido,K., Ishii,S. and Komiyaba,N. (1989) *Nucleic Acids Res*., **17**, 9749–9759.
16 Krude,T. and Knippers,R. (1991) *Mol. Cell. Biol*., **11**, 6257–6267.
17 Kanaar,R., Klippel,A., Shekhtman,E., Dungan,J.M., Kahmann,R. and Cozzarelli,N.R. (1990) *Cell*, **62**, 353–366.
18 Smith,C.L., Matsumoto,T., Niwa,O., Klco,S., Fan,J.B., Yanagida,M. and Cantor,C.R. (1987) *Nucleic Acids Res*., **15**, 4481–4489.
19 Schwartz,D.C. and Cantor,C.R. (1984) *Cell*, **37**, 67–75.

20 Sanseau,P., Tiffoche,C., Kahloun,A.-E., Collin,O., Rolland,J.-P. and Le Pennec,J.P. (1990) *Anal. Biochem.*, **189**, 142–148.
21 Carle,G.F. and Olson,M.V. (1984) *Nucleic Acids Res.*, **12**, 5647–5664.
22 Carle,G.F., Frank,M. and Olson,M.V. (1986) *Science*, **232**, 65–68.
23 Chu,G., Vollrath,D. and Davis,R.W. (1986) *Science*, **234**, 1582–1585.
24 Peck,L.J. and Wang,J.C. (1983) *Cold Spring Harbor Symp. Quant. Biol.*, **47**, 85–91.
25 Kornberg,A. and Baker,T.A. (1992) *DNA Replication*, 2nd. Edn. W.H.Freeman and Co., New York, NY.
26 Brewer,B.J., Sena,E.P. and Fangman,W.L. (1988) *Cancer Cells*, **6**, 229–234.
27 Schvartzman,J.B., Adolph,S., Martín-Parras,L. and Schildkraut,C.L. (1990) *Mol. Cell. Biol.*, **10**, 3078–3086.
28 Clewell,B.D. and Helinski,D.R. (1969) *Proc. Natl. Acad. Sci. USA*, **62**, 1159–1166.
29 Sambrook,J., Fritsch,E.F. and Maniatis,T. (1989) *Molecular Cloning: A Laboratory Manual*, 2nd Edn. Cold Spring Harbor Laboratory Press, Cold Spring Harbor, NY.
30 Blow,J.J. and Laskey,R.A. (1986) *Cell*, **47**(4), 577–587.
31 Murray,A.W. (ed.) (1991) In Kay,B.K. and Peng,H.B. (eds), *Methods in Cell Biology*, Vol. 36, *Cell Cycle Extracts*. Academic Press, San Diego, CA.
32 Sharp,P.A., Sugden,B. and Sambrook,J. (1973) *Biochemistry*, **12**, 3055–3063.
33 Bauer,W. and Vinograd,J. (1968) *J. Mol. Biol.*, **33**, 141–171.
34 Stasiak,A., Katrich,V., Bednar,J., Michoud,D. and Dubochet,J. (1996) *Nature*, **384**, 122.
35 Wasserman,S.A., Dungan,J.M. and Cozzarelli,N.R. (1985) *Science*, **229**, 171–174.
36 Kreuzer,K.N. and Cozzarelli,N.R. (1980) *Cell*, **20**, 245–254.
37 Crisona,N.J., Kanaar,R., Gonzalez,T.N., Zechiedrich,E.L., Klippel,A. and Cozzarelli,N.R. (1994) *J. Mol. Biol.*, **243**, 437–457.
38 Katrich,V., Bednar,J., Michoud,D., Scharein,R.G., Dubochet,J. and Stasiak,A. (1996) *Nature*, **384**, 142–145.
39 Sanchez,J.A., Wonsey,D.R., Harris,L., Morales,J. and Wangh,L.J. (1995) *J. Biol. Chem.*, **270**, 29676–29681.
40 Hirano,T. and Mitchison,T.J. (1991) *J. Cell. Biol.*, **115**, 1479–1489.
41 Luke,M. and Bogenhagen,D.F. (1989) *Dev. Biol.*, **136**, 459–468.
42 Newport,J. (1987) *Cell*, **46**, 205–217.
43 Kavenoff,R., Klotz,L.C. and Zimm,B.H. (1974) *Cold Spring Harbor Symp. Quant. Biol.*, **38**, 1–8.
44 Sasaki,M.S. and Norman,A. (1966) *Exp. Cell Res.*, **44**, 642–645.
45 Sikorav,J.L. and Jannink,G. (1994) *Biophys. J.*, **66**, 827–837.
46 van den Engh,G., Sachs,R. and Trask,B.J. (1992) *Science*, **257**, 1410–1412.
47 Cairns,J. (1963) *J. Mol. Biol.*, **6**, 208–213.
48 Ullsperger,C.J., Vologodskii,A.V. and Cozzarelli,N.R. (1995) In Lilley,D.M.J. and Eckstein,F. (eds), *Nucleic Acids and Molecular Biology*, Vol. 9, *Unlinking of DNA by Topoisomerases during DNA Replication*. Springer-Verlag, Berlin, Germany.
49 Weaver,D.T., Fields-Berry,S.C. and DePamphilis,M.L. (1985) *Cell*, **41**, 565–575.
50 Martín-Parras,L., Hernández,P., Martínez-Robles,M.L. and Schvartzman,J.B. (1992) *J. Biol. Chem.*, **267**, 22496–22505.
51 Belanger,K.G., Mirzayan,C., Kreuzer,H.E., Alberts,B.M. and Kreuzer,K.N. (1996) *Nucleic Acids Res.*, **24**, 2166–2175.
52 Preiser,P.R., Wilson,R.J., Moore,P.W., McCready,S., Hajibagheri,M.A., Blight,K.J., Strath,M. and Williamson,D.H. (1996) *EMBO J.*, **15**, 684–693.